Proceedings of the Institute of Acoustics

DETERMINATION OF THE TIME OF ENERGY RETURN FROM BEAMFORMED DATA

E J Kaminsky (1), A B Martinez (2), B S Bourgeois (3), C Zabounidis (4) & W J Capell (4)

(1) Sverdrup Technology, Stennis Space Center, MS, USA.
(2) Tulane University, EE Dept., New Orleans, LA, USA.
(3) Naval Research Lab., Stennis Space Center, MS, USA.
(4) SeaBeam Instruments, Inc., Westwood, MA, USA.

1. INTRODUCTION

Multibeam bathymetric sonar systems such as the Sonar Array Survey System (SASS), the Sea Beam, and the Sea Beam 2000, are capable of collecting data which, after proper processing, may be used to map the bottom of the ocean. The sonar energy from the projector array impinges the ocean bottom as a narrow swath perpendicular to the ship's heading. The echo from this swath is received by an array of hydrophones mounted athwartships. Beamforming permits good reception of energy propagating in a certain direction while attenuating energy propagating in other directions, and may be performed in hardware or software. Beamformed data gives a time history of the energy received from each look direction ϕ_k. This data must be further processed to determine the time corresponding to the center of the beam, t_c. The peak of the envelope corresponds to the intersection of the Maximum Response Axis (MRA) of the beam and the area ensonified. Once the time t_c has been determined, the bathymetry of the area surveyed can be obtained.

In [1] simulation was used to determine the performance of recursive filters matched to a Gaussian bottom return signal to find t_c. A Rician model for the bottom return signals and nonrecursive digital matched filters were used in [2]. In this paper, we study several methods that might be used for determining the time t_c of energy return for each bin. These methods are matched filtering detection, peak detection and Weighted Mean Time (WMT). Synthetic data generated using Morgera's models for the bottom return signal are used to compare the performance of these methods as regards accuracy, bias, angular dependency of their performance, and computational efficiency. Comparisons of the algorithms applied to actual survey data collected by SASS are also presented, and show acceptable performance of all algorithms tested.

2. BEAM CENTER DETECTION

The area ensonified by the intersection of the transmit and receive beams produces an echo return from which bathymetry must be extracted. This area typically increases with increasing steering angle ϕ, and the returned energy spans a finite time. The acoustic signals reflected from a wide swath beneath the ship are spatially separated into beams by the beamformer. Time–of–arrival data are obtained from the beam signals. A detector is used to determine which point in the time envelope corresponds to the bottom. Determination of this time should be easier for the narrow high Signal–to–Noise Ratio (SNR) nadir returns than for the noisier and wider pulses from higher angles. If ideal conditions were present the peak of the energy signal returned for each beam would correspond to the MRA of the beam. Actual conditions include noise and signal fluctuations. Weighted Mean Time (WMT) algorithms (center of mass) have been used by Sea Beam and Sea Beam 2000. Matched filtering has been used for SASS [3]. Simple peak detection may also be used. These methods are reviewed in this section.

The simplest way of determining the time corresponding to the MRA of the bottom return signal is to use a peak detector. It finds the largest amplitude of the signal and then determines the sample time for which this return occurred.

With matched filtering, filters loosely matched to the return signal are generated, a filtering operation is

performed, and the peak of the signal at the output of the filter is then detected. Observation of data collected by SASS indicate a roughly Gaussian shape of the returned signal for all steering angles. The impulse response of the filters generated are made Gaussian as well to provide a relatively close match to the returned energy. The width w of the filter can be predetermined or computed from the data collected. The Gaussian matched filter is created from samples of

$$y = \exp\left[-\frac{1}{2}\left(\frac{x}{\sigma}\right)^2\right] \tag{1}$$

The signal obtained for each beamformer bin is convolved with its matched filter, and a smoother signal is obtained. Filtering also emphasizes the peak so that peak detection can then be used. The main disadvantage of using Gaussian filters is that convolutions must be performed; this is very time consuming and might therefore preclude its use for real–time processing. If the Gaussian filter is replaced by a filter with a rectangular impulse response, a much simpler filter is obtained at the expense of a worse match to the return signal. When rectangular filters are used convolutions are not required.

In Sea Beam's operation, the echo processor digitizes the echo envelopes and applies ray bending, roll and gain corrections, and sidelobe suppression. A time of arrival is then determined at the center of mass of each of the 16 corrected echoes [4, 5]. Sea Beam weighs every time sample by its amplitude (the voltage V_i) as in (2), while Sea Beam 2000 uses powers as in (3). The Sea Beam systems use exclusively the WMT algorithm for bottom detection on the entire swath. The Sea Beam 2000 uses WMT only on the portions of the swath that correspond to near vertical returns; for the rest of the swath an interferometric detection process is applied. The interferometric detection method is in general more accurate than WMT, but is not discussed in this paper.

$$t_c = \frac{\sum_{i=i_{min}}^{i_{max}} V_i t_i}{\sum_{i=i_{min}}^{i_{max}} V_i} \tag{2}$$

$$t_c = \frac{\sum_{i=i_{min}}^{i_{max}} P_i t_i}{\sum_{i=i_{min}}^{i_{max}} P_i} \tag{3}$$

Adaptive thresholding[1] is performed prior to the determination of the time corresponding to the MRA of the beam, in order to separate actual responses from dropouts and noise. This should be done regardless of the detection method used to avoid processing useless data, but is specially important for the WMT algorithms. The window used determines i_{min} and i_{max}.

3. SIMULATIONS

Numerous Monte Carlo simulations were performed to reliably (at least 90% confidence) compare the different MRA time detection methods. The algorithms were applied both to the voltage signals and to the intensity (power) signals. Although sufficient survey data from operating systems are available for this study, the actual location of the peaks, t_c, is unknown. For simulation purposes, then, Gaussian and Rician models from [1, 2] were used to generate the simulated bottom return of which the actual peak time is known. In both cases the generated smooth–bottom return is corrupted by multiplicative and additive low–pass filtered white Gaussian noises. The models were presented in [1, 2] and are simply summarized here for continuity.

[1] Sea Beam's thresholding method is proprietary information.

TIME OF ENERGY RETURN

The simulated bottom return signal at time sample k, is

$$b(k) = s(k) \cdot n_1(k) + n_2(k) \tag{4}$$

where n_1 and n_2 are the output of digital third order Butterworth filters with cutoff frequencies W_1 and W_2 Hz, respectively, when the inputs are white Gaussian noise sequences of mean zero and standard deviations σ_1 and σ_2. The variance σ_1^2 of the multiplicative noise controls the level of the signal and the bandwidth W_1 sets the fluctuation rate of the signal $b(k)$. The variance σ_2^2 controls the additive noise level, while W_2 determines its bandwidth. The parameters combine to determine the SNR as given in (5).

$$SNR = 20 \log_{10} \left[\frac{\sigma_1}{\sigma_2} \left(\frac{W_1}{W_2} \right)^{1/2} \right] \tag{5}$$

Morgera first modelled the noiseless signal $s(k)$ from (4) as a Gaussian signal and then as an approximation to the functional form of the Rician pdf. These signals are given in (6) and (7), respectively.

$$s(k) = \exp \left[-\frac{\pi^2 t^2(k)}{T^2 4 \ln 2} \right] \tag{6}$$

$$s(k) = \begin{cases} \frac{r}{\sigma^2} \exp\left(-\frac{r^2}{2\sigma^2}\right), & S \ll 1 \\ \frac{1}{\sqrt{2\pi}\sigma} \exp\left[-\frac{(r-E_c)^2}{2\sigma^2}\right] & S \gg 1 \end{cases} \tag{7}$$

where $S = \frac{E_c^2}{2\sigma^2}$. The parameters E_c and σ in (7) were chosen to be

$$E_c = \tau \left[\exp(\cos\phi) - 1 \right] \tag{8}$$

$$\sigma = \alpha T(\phi, d) \tag{9}$$

where the approximate values of α used are 0.6 close to nadir and 0.8 off nadir. T is the expected echo duration given by

$$T(\phi, d) \approx \frac{2d\theta}{c} \tan\phi \sec\phi + \tau \tag{10}$$

with d the depth, ϕ the steering angle, c the speed of sound in water, τ the time duration of the transmitted signal, and θ the receive beamwidth in radians. The parameters in Morgera's models were chosen to resemble those of SASS data and are given in Table 1.Figure 1 shows normalized Rician and Gaussian signals $s(k)$ and the noisy bottom returns $b(k)$ for a SNR of 15 dB and angle ϕ of 30 degrees.

A major difference between Morgera's work and ours is that we maintain a constant sampling rate regardless of the angle ϕ. Morgera uses a constant number of samples per "hump", therefore using a much higher sampling rate for angles close to nadir than for angles close to endfire; actual operating systems typically maintain a constant sampling rate.

We chose to define the width w of the matched filters from $\sigma = \frac{w}{6}$, where w needs to be determined. It can either be based on the SNR (data dependent threshold) or on the expected width of the return, which is easily computed from (10) where a flat bottom assumption was made. In our simulations we compute w as the number of samples that exceed a threshold set to twice the standard deviation of the returned noisy signal for the Gaussian filters, and 2.5 times the standard deviation in the case of the rectangular filters. When using (1), the independent variable ranged from -100 to 100.

TIME OF ENERGY RETURN

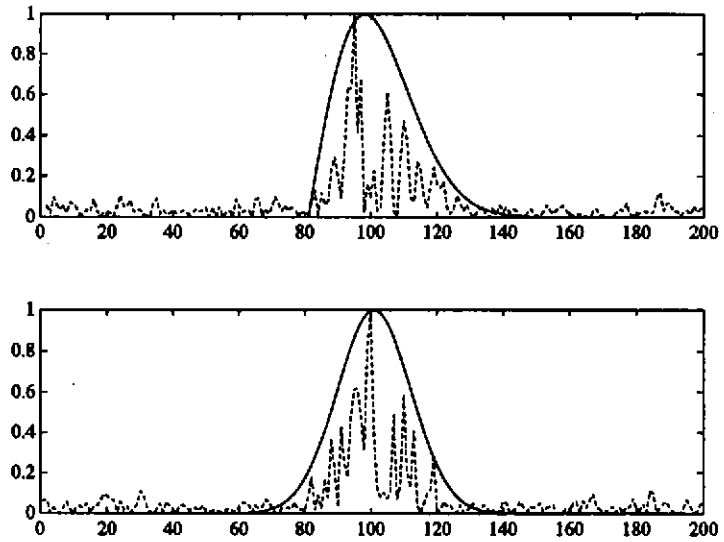

Figure 1: Ideal and noisy Rician (top) and Gaussian (bottom) returns.

Table 1: Value of Parameters used for Simulations.

Parameter	Value	Parameter	Value
θ	1°	d	12000 ft
W_1	140 Hz	W_2	420 Hz
τ	.007 s	c	4895 ft/s
f_s	333.3 Hz	n	1024

4. RESULTS

Two large sets of results were obtained during this study. The first set is from signals generated using the modelled returns; the second is from SASS signals. For the simulated signals, a number of noisy bottom returns were generated according to (4) for a given SNR and angle. These returns were pre–processed to detect dropouts. It is determined that a droupout exists when the corresponding width of the filter is very wide (over 200 samples), or when the width is relatively wide for a narrow angle and at the same time the maximum return is smaller than four times the threshold used for width determination. The signals that passed the threshold were processed with the different algorithms to determine the center time. The statistics that characterize the performance of the detection methods were then computed from a large number (enough for 90% confidence) of simulations. The standard SASS processing [3] was applied to the SASS survey samples to obtain the results for this set of data. The survey data were processed only by the peak detector and the Gaussian and rectangular filters.

Figure 2 shows results of the Monte Carlo simulations (1000 runs) for a SNR of 15 dB and an angle ϕ of 30 degrees for a Rician pulse with peak at 515. Plots a) through f) are for Gaussian filter, peak detection, rectangular filter, WMT on voltage, WMT on power, and Gaussian filter on power, respectively. It is clear we would like these pdfs to be centered around the correct time (515), be very narrow, and have the largest frequency at the correct time. The results for Gaussian filtering and peak detection show that the correct time is chosen most often with those algorithms, but that many other times are sometimes selected, making

the variance relatively large. The results obtained with the WMT algorithms show a very small variance, but a marked (and expected) bias of the results. From Fig. 2 we also see that the rectangular filters yield small biases (± 1) with large variances, while the results of the Gaussian filters and peak detection are unbiased with similar variances. Notice, though, that the correct center time is chosen less than 20% of the time.

Results for the Gaussian–shaped pulses at 30 degrees and for all SNR tested generate Gaussian–like pdfs centered at the correct time, and with variances smaller than those obtained for Rician pulses. The WMT algorithm applied to the voltage signal detects the correct time over 50% of the time for a SNR as low as 5 dB, with a very small variance. A large number of combinations of angles and SNR were simulated. In

Table 2: Beam Center Time Results for $\phi = 15^0$

Algorithm	Signal Shape	SNR = 20 dB				SNR= 10 dB			
		t_c	ext	σ	m,%	t_c	ext	σ	m,%
Gaussian on signal.	Rician	1.0	22	1.6	1,24	1.5	17	1.8	1,26
	Gaussian	0.0	24	1.7	0,24	0.1	28	1.7	0,28
Rectangular on signal	Rician	1.2	21	1.3	1,32	2.2	8	4.0	2,13
	Gaussian	-0.3	23	1.6	0,23	-0.2	16	3.5	0,16
Peak detection	Rician	0.6	13	3	1,14	0.7	15	2.6	0,15
	Gaussian	0.1	15	2.7	0,15	-0.1	12	2.8	0,12
Gaussian on Power	Rician	1.6	15	2.3	1,15	0.8	20	1.8	1,21
	Gaussian	0.1	15	2.4	0,15	0.0	20	2.0	0,20
Rectangular on Power	Rician	.5	22	1.8	0,22	0.8	21	1.9	1,21
	Gaussian	-0.3	21	1.9	0,21	-0.2	20	2.0	0,20
WMT on signal	Rician	1.3	11	0.7	1,47	1.0	21	0.73	1,53
	Gaussian					0.0	50	0.76	0,50
WMT on power	Rician	1.1	24	1.1	1,35	1.0	22	1.1	1,38
	Gaussian					0.0	35	1.1	0,35

Table 3: Beam Center Time Results for $\phi = 45^0$

Algorithm	Signal Shape	SNR = 20 dB				SNR= 10 dB			
		t_c	ext	σ	m,%	t_c	ext	σ	m,%
Gaussian on signal.	Rician	1.8	7	6.4	2,8	2.2	8	5.7	2,7
	Gaussian	-.4	6	6.0	0,6	0.0	7	5.1	0,7
Rectangular on signal	Rician	2.1	7	5.4	2,6	2.0	6	5.9	2,6
	Gaussian	-0.2	8	5.5	0,8	-0.2	7	5.9	0,7
Peak detection	Rician	1.5	4	9.7	1,3	1.3	4	10.1	1,4
	Gaussian	-0.3	5	8.7	0,5	0.0	4	9.1	0,4
Gaussian on Power	Rician	1.3	5	8.1	1,4	1.6	4	8.5	2,4
	Gaussian	-0.5	6	7.7	0,6	0.1	5	7.5	0,5
Rectangular on Power	Rician	1.0	5	7.2	1,6	1.2	5	7.3	2,4
	Gaussian	-0.5	5	6.8	0,5	-0.3	5	6.8	0,5
WMT on signal	Rician	5.9	0	1.5	6,NA	4.4	0	1.5	4,NA
	Gaussian	0.0	25	1.5	0,25	0.1	25	1.6	0,25
WMT on power	Rician	4.3	3	2.3	4,NA	4.1	4	2.4	4,NA
	Gaussian	0.0	20	2.3	0,20	0.1	17	2.3	0,17

Tables 2 and 3 we show the difference (in sample counts) between the time of the peak, t_c, and the time selected as the MRA time by the various algorithms for look directions of 15 and 45 degrees, respectively, and SNR of 20 and 10 dB. Results for both Rician– and Gaussian–shaped pulses are given. The percentage of time the exact peak time was correctly detected (ext), the standard deviation (σ), and the median value (m) together with the percentage of time the median value occurred are also shown.

TIME OF ENERGY RETURN

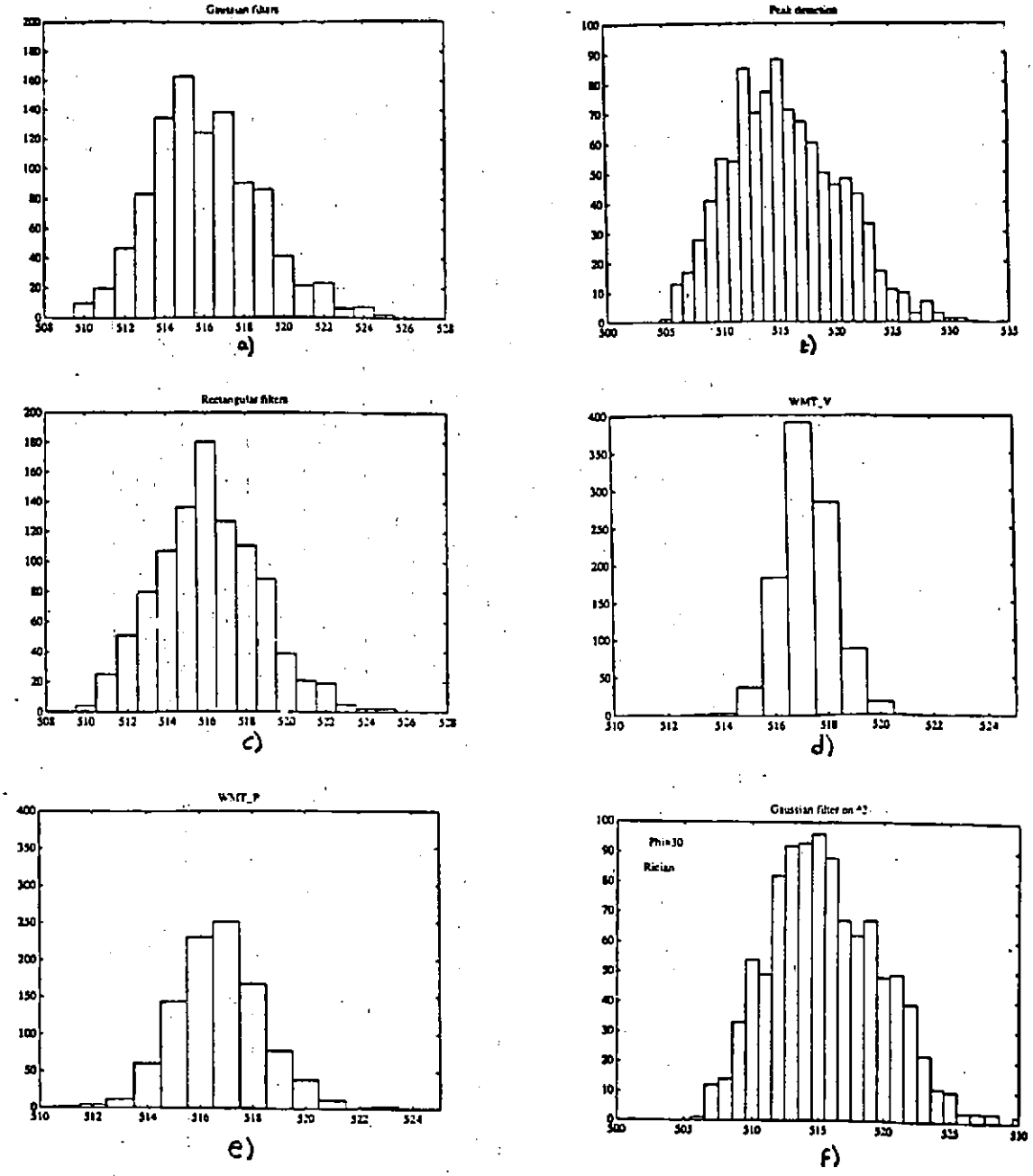

Figure 2: Pdfs for Rician signal with SNR of 15 dB and angle of 30 degrees.

TIME OF ENERGY RETURN

The results are somewhat dependent upon parameters such as the threshold level used to determine the width of the filter, but we tried to minimize these dependencies. Windowing to reduce sidelobes also has some effect on the results obtained. When no windowing was used and therefore the sidelobes of the specular return appeared as a high intensity at other angles, the Gaussian matched filter algorithm performed better than peak detection, selectin the (erroneous) sidelobe less frequently.

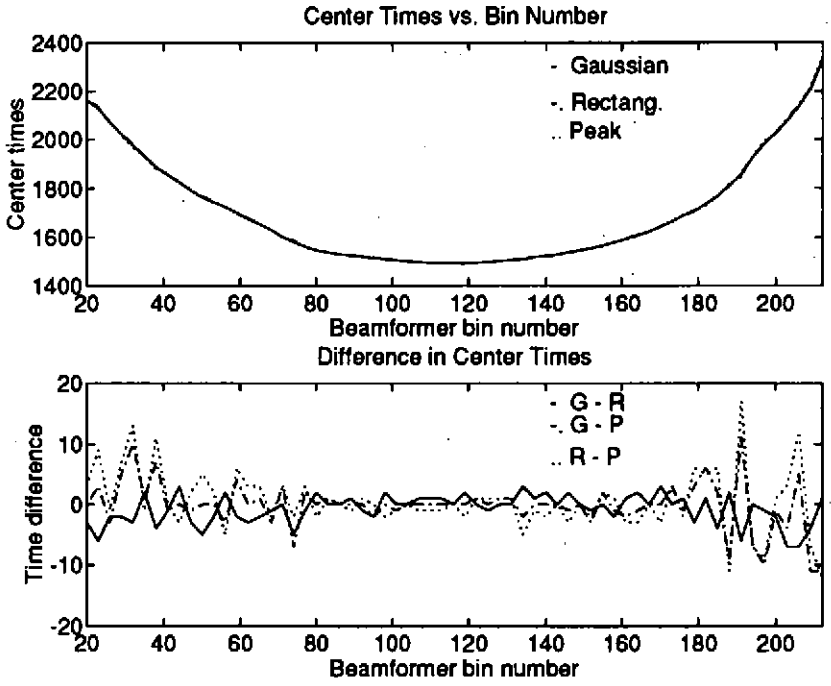

Figure 3: Comparison results on survey data from SASS.

In Fig. 3 we show some results for peak detection, Gaussian and rectangular filtering when applied to a typical ping of SASS data. The center times, in sample number, are plotted at the top of Fig. 3. The difference between results from the three algorithms are too small to be seen in this plot. In the bottom of Fig. 3 the difference, also in number of samples, is plotted versus the beamformer bin number. We see that although the differences are small for angles close to nadir, these increase as the steering angle aproaches the extremes. The average difference in the resulting bathymetry for the data shown in Fig. 3 is about .25% of the depth with the worst case difference being about 1.5% of the depth. Remember that for this data we don't have the actual correct t_c, and only comparison between the yielded results are possible.

5. CONCLUSIONS AND SUGGESTIONS

Results show that the actual shape of the energy pulses discriminated angularly markedly affects the results, and must therefore be investigated further. The noise characteristics and statistics must also be studied.

We showed here that all algorithms presented perform well, including simple peak detection, especially if some pre–processing is performed to determine dropouts and eliminate sidelobes. The Weighted Mean Time algorithms were shown to yield results with very narrow distributions, although they produce biased

estimates if the return pulse is not symmetric. We suggest that if very accurate determination of the center of the peak must be made, the estimate produced by a peak detector can be used to place the window and then the Weighted Mean Time algorithm can be applied to the windowed data to obtain the final center time; this estimate might need to be de-biased.

Another area that needs to be investigated is the accuracy of the velocity profiles and the effect that errors in them cause on the resulting bathymetry. If errors caused by lack of exact profiles for ray bending calculations are considerable, it might be senseless to try to obtain an exact MRA time. If this is the case, simple peak detection is certainly a method to consider.

6. ACKNOWLEDGMENTS

The authors acknowledge the Office of Naval Technology, project element 602435N, managed by Dr. Herbert C. Eppert, Jr., NRL, Stennis Space Center, MS. This paper, NRL Contribution Number NRL/PP/7441-93-0011, is approved for public release; distribution is unlimited.

References

[1] S. D. Morgera, "Signal processing for precise ocean mapping," *IEEE J. Oceanic Engineering*, vol. OE-1, pp. 49–52, November 1976.

[2] S. D. Morgera and R. Sankar, "Digital signal processing for precision wide-swath bathymetry," *IEEE J. Oceanic Engineering*, vol. OE-9, pp. 73–84, April 1984.

[3] E. J. Kaminsky, B. S. Bourgeois, A. B. Martinez, and H. Barad, "SASS imagery development," Technical Report in process, NRL, Code 351, Sept. 1992.

[4] H. K. Farr, "Multibeam bathymetric sonar: Sea Beam and Hydrochart," *Marine Geodesy*, vol. 4, no. 2, pp. 289–298, 1980.

[5] C. de Moustier, "Beyond bathymetry: Mapping acoustic backscattering from the deep seafloor with Sea Beam," *Journal of the Acoustical Society of America*, vol. 79, pp. 316–331, February 1986.